HHS Public Access

Author manuscript

J Biomed Mater Res B Appl Biomater. Author manuscript; available in PMC 2020 July 01.

Published in final edited form as:

J Biomed Mater Res B Appl Biomater. 2019 July ; 107(5): 1576–1586. doi:10.1002/jbm.b.34250.

A novel patient-specific three-dimensional drug delivery construct for regenerative endodontics

Marco C. Bottino[a,*], **Maria T. P. Albuquerque**[b], **Asma Azabi**[c], **Eliseu A. Münchow**[d], **Kenneth J. Spolnik**[e], **Jacques E. Nör**[a], and **Paul C. Edwards**[f]

[a]Department of Cariology, Restorative Sciences and Endodontics, University of Michigan School of Dentistry, Ann Arbor, MI - 48109, USA.

[b]Department of Clinical Dentistry (Endodontics), Federal University of Bahia, Salvador, BA - 40110, Brazil.

[c]Department of Biomedical & Applied Sciences, Indiana University School of Dentistry (IUSD), Indianapolis, IN - 46202, USA.

[d]Department of Dentistry, Health Science Institute, Federal University of Juiz de Fora, Governador Valadares, MG - 35010, Brazil.

[e]Department of Endodontics, IUSD, Indianapolis, IN - 46202, USA.

[f]Department of Oral Pathology, Medicine, and Radiology, IUSD, Indianapolis, IN - 46202, USA.

Abstract

Evoked bleeding (EB) clinical procedure, comprising a disinfection step followed by periapical tissue laceration to induce the ingrowth of undifferentiated stem cells from the periodontal ligament and alveolar bone, is currently the only regenerative-based therapeutic approach to treating pulp tissue necrosis in undeveloped (immature) permanent teeth approved in the United States. Yet, the disinfection step using antibiotic-based pastes leads to cytotoxic, warranting a biocompatible strategy to promote root canal disinfection with no or minimal side-effects to maximize the regenerative outcomes. The purpose of this investigation was to develop a tubular three-dimensional (3D) triple antibiotic-eluting construct for intracanal drug delivery. Morphological (scanning electron microscopy), chemical (Fourier transform infrared spectroscopy), and mechanical (tensile testing) characteristics of the polydioxanone-based triple antibiotic-eluting fibers were assessed. The antimicrobial properties of the tubular 3D constructs were determined *in vitro* and *in vivo* using an infected (*Actinomyces naeslundii*) dentin tooth slice model and a canine method of periapical disease, respectively. The *in vitro* data indicated significant antimicrobial activity and the ability to eliminate bacterial biofilm inside dentinal tubules. *In vivo* histological findings demonstrated that, using the EB procedure, the tubular 3D triple antibiotic-eluting construct allowed the formation of an appropriate environment that led to apex closure and the ingrowth of a thin layer of osteodentin-like tissue into the root canal. Taken

[*]**Corresponding author at:** University of Michigan School of Dentistry, Department of Cariology, Restorative Sciences and Endodontics, 1011 N. University (Room 5223), Ann Arbor, MI - 48109, USA. Tel: +1-734.763.2206 Fax: +1-734.936.1597. mbottino@umich.edu (Dr. Marco C. Bottino).

together, these findings indicate that our novel drug delivery construct is a promising biocompatible disinfection strategy for immature permanent teeth with necrotic pulps.

Keywords

electrospinning; nanofibers; drug delivery; disinfection; regeneration; endodontics

INTRODUCTION

Dental pulp, a highly vascularized and innervated non-mineralized tissue, plays a vital role in tooth development as it harbors progenitor cells that proliferate and differentiate into dentin-secreting odontoblasts.[1] From a physiological standpoint, the pulp provides nutritive, sensory, formative, and defensive abilities to the tooth.[2] Preserving pulp vitality ensures tooth development and the stimulation of tertiary dentin formation following injury and proper immune response to block bacterial infection.[2] Regretably, pulpal inflammation and eventual necrosis are likely to occur due to traumatic injuries or dental caries.[3] Upon recurrent and persistent bacterial insult, the pulp undergoes chronic irreversible inflammation, ultimately leading to necrosis. Nearly 20% of school children in the United States experience some kind of dental trauma[4], which may directly affect pulp nourishment due to apical blood vasculature damage.[5]

Root canal therapy involving debridement, instrumentation, and obturation of the pulp canal space is the current treatment of choice to achieve tight apical sealing in fully-developed necrotic permanent teeth.[6] However, given the wide, open apical foramen and thin dentinal walls exhibited by immature permanent teeth in children aged 6 to mid-teens, traditional endodontic therapy is not advisable.[7] Instead, the necrotic pulp tissue is extirpated and the root canal space is cleaned prior to a clinical procedure termed apexification.[3] Apexification relies on the use of calcium hydroxide or mineral trioxide aggregate (MTA) to induce the formation of a mineralized barrier, resulting in the closure of the apical foramen.[8] However, apexification only resolves the symptoms of pathosis[3]; it does not restore the immunocompetence of the pulp nor support continued root development[9], increasing the risk of tooth loss following re-infection or secondary trauma.[3]

Numerous researchers have sought clinical alternatives to treat permanent teeth with necrotic pulps[7, 10–13], but to date, only a few case reports[14,15] have evidenced the formation of a pulp-like tissue following the EB approach. Clinically, regenerative endodontics aims to engineering a metabolically active and blood carrying dental pulp capable of forming new dentin.[16–18] The lack of progress, despite significant advancements on potentially translatable strategies, may be attributed to the intracanal placement of cytotoxic highly concentrated antibiotic pastes (e.g., triple antibiotic paste – equal parts, i.e., 1 g/mL in total of three antibiotics metronidazole/MET, ciprofloxacin/CIP, and minocycline/MINO)[19] during the most critical phase of the EB method (i.e., disinfection), the difficulty in its removal[20], and likely interference with the release of growth factors from dentin.[21] Thus, it is paramount to develop a more cell-friendly disinfection method in addition to a predictable pulp-dentin complex regeneration strategy, reducing the risk of re-infection and ultimately

leading to the establishment of novel therapeutics to treat permanent teeth with necrotic pulps.[22,23]

In pursuing the development of a clinically viable, biocompatible disinfection method, our group was the first to establish a strategy through the use of antibiotic-eluting polymer nanofibers capable of eradicating dentin biofilm with minimal toxicity to dental pulp stem cells.[24–27] In the present work, we demonstrate, for the first time, the clinical role of a biocompatible triple antibiotic (MET, CIP, and MINO) 3D drug delivery construct when associated with EB using a canine model of periapical disease.

MATERIALS AND METHODS

Synthesis and characterization of tubular 3D drug delivery constructs.

The synthesis of antibiotic-eluting fibers for drug delivery was performed following previously optimized electrospinning parameters[28,29] to obtain tubular 3D constructs. In brief, polydioxanone (PDSII®, Ethicon, Somerville, NJ, USA) was procured in the form of Food and Drug Administration (FDA) approved biodegradable sutures. The purple dye was removed from the suture filaments by soaking in a glass flask containing dichloromethane (Sigma, St. Louis, MO, USA) for 48 h, followed by vacuum drying for 24 h to aid in solvent evaporation.[24] Next, undyed filaments were solubilized in 1,1,1,3,3,3-hexafluoro-2-propanol (HFP, Sigma) to obtain a spinnable solution (100 $mg.ml^{-1}$). Three antibiotics (Sigma) namely metronidazole (MET), ciprofloxacin (CIP), and minocycline (MINO) commonly employed in the formulation of the so-called triple antibiotic paste (TAP) and widely used to disinfect immature permanent teeth with necrotic pulps, were incorporated into the polymer solution (35 mg of each antibiotic per ml of the polymer solution) based on previously reported data demonstrating minimal cell toxicity and significant antimicrobial efficacy against different endodontic pathogens.[24–27] Antibiotic-free polymer solution was also prepared. After overnight stirring, each solution was loaded into 5 ml plastic syringe (Becton, Dickinson and Company, Franklin Lakes, NJ, USA) with a metallic 27-gauge blunt tip needle. The syringe and needle were placed in a syringe pump (Legato 200, KD Scientific Inc., Holliston, MA, USA) to be dispensed at 2 $ml.h^{-1}$ and 18 cm distance from the tip of the needle to the target, a cylindrical grounded 1.5 mm in diameter Teflon®-coated steel mandrel connected to a mechanical stirrer (BDC6015, Caframo, Wiarton, ON, Canada). The solutions were electrospun onto the mandrel (120 rpm) at an applied voltage of +15 kV and +19 kV (ES50P-10W/DAM, Gamma High-Voltage Research Inc., FL, USA) to obtain tubular 3D antibiotic-free (AF-$3D_C$) and triple antibiotic-eluting (TA-$3D_C$) constructs (Fig. 1). The constructs were then dried for 48 h under vacuum and stored at 4°C until use.[29]

Morphological characterization.

Electrospun fibers were observed using a field emission scanning electron microscope (FE-SEM, JSM-6701F, JEOL, Tokyo, Japan). Briefly, samples taken from antibiotic-free and triple antibiotic-eluting fibers were mounted on Al stubs using double-sided carbon adhesive tape and sputter-coated with Au-Pd prior to imaging. Fiber diameter and distribution were obtained with ImageJ software (National Institutes of Health, Bethesda, MD, USA). Mean

fiber diameter was calculated and reported (mean±SD) based on the measurement of 150 single-fibers (50 randomly chosen measurements per image) at the same magnification (5000×).[24]

Chemical analysis.

To confirm the incorporation of MET, CIP, and MINO into the fibers, attenuated total reflectance–Fourier transform infrared spectroscopy (ATR–FTIR) was carried out (Jasco FTIR-4100, Easton, MD, USA). Measurements were taken in the range of 4000–700 cm^{-1} at a resolution of 4 cm^{-1} with 128 scans.[24]

Mechanical properties.

Mechanical properties (i.e., tensile strength, Young's modulus, and elongation at break) of the fibers were evaluated by uni-axial tensile testing (expert 5601, ADMET, Norwood, MA, USA). Thickness of rectangular samples (15 × 3 mm^2) was determined at three locations using calipers. The specimens were tested (n=10/group/condition) both under dry and wet (24 h incubation in phosphate-buffered saline; PBS) conditions at a crosshead speed of 1 $mm.min^{-1}$.[30] Mechanical data were obtained from the load-displacement curves and expressed in MPa. The results are reported as mean±SD. Data were analyzed using Two-Way Analysis of Variance (ANOVA) and Tukey's test for multiple comparison (α=0.05) (SigmaPlot version 12, Systat Software Inc., San Jose, CA, USA).

Infected dentin tooth slice model – *In vitro*.

To assess the antimicrobial efficacy of the tubular 3D triple antibiotic-eluting constructs, a clinically relevant *in vitro* infected dentin tooth slice model was developed. In brief, *Actinomyces naeslundii* (*An*), a gram-positive filamentous, rod-shaped facultative anaerobe[31] was chosen to form a 7-day old biofilm inside dentinal tubules of dentin slices (Fig. 2). Twenty-four caries-free human canines, collected based on a local (Indiana University, Indianapolis, IN, USA) Institutional Review Board protocol (protocol #1407656657), were used to prepare 1-mm thick dentin slices. After removal from the storage medium (Thymol 0.1%, Sigma-Aldrich), the teeth were thoroughly cleaned with ultrasonic scalers prior to crown sectioning using a low-speed water-cooled diamond blade (Isomet, Buehler, Lake Bluff, IL, USA). The roots were then horizontally sectioned at 3-mm apical to the cement-enamel junction (CEJ) to obtain 1.5 ± 0.1-mm thick dentin slices that were further standardized to 1-mm thick slices (Fig. 2A) via wet-finishing with silicon carbide papers (Buehler). A round (ϕ = 2.5 mm) carbide bur was used at low speed (300 rpm) under water-cooling to standardize the root canals of the dentin slices. To remove the smear layer, dentin slices were incubated in an ultrasonic bath of 2.5% sodium hypochlorite (NaOCl), followed by 17% ethylenediaminetetraacetic acid (EDTA; Inter-Med, Inc., Racine, WI, USA) for 3 min each. Dentin slices were rinsed in saline solution for 10 min and autoclaved at 121°C.[32]

Dentin slices were randomly and individually placed in sterile centrifuge tubes containing 500 µl of *A. naeslundii* suspension (~10^6 bacteria) and centrifuged to allow bacterial penetration inside dentinal tubules. In brief, a sequence of centrifugal cycles at 1400 g, 2000 g, 3600 g, and 5600 g for 5 min (2× each) was performed.[33] The bacterial suspension was

refreshed between every centrifugation cycle. The infected slices (one per well) were then distributed to 24-well plates containing 1 ml of BHI (brain heart infusion broth) + 1% sucrose (BHIS). The plates were then incubated in aerobic conditions at 37°C and 5% CO_2 for 7 days for biofilm formation (Fig. 2B). BHIS was replaced every other day to remove detached cells and ensure cell viability. After 7 days of anaerobic culture, the dentin slices were gently rinsed with sterile PBS to remove the culture medium and non-adherent bacterial cells. Then, 6 infected slices were randomly allocated into the following groups: negative control (7-day biofilm), antibiotic-free 3D construct (AF-$3D_C$), triple antibiotic-eluting 3D construct (TA-$3D_C$, fabricated as explained in 2.1.) and positive control (triple antibiotic paste, TAP). Tubular 3D constructs were sterilized by UV-irradiation (30 min per side) and fitted inside the infected root canal space (Fig. 2A). Meanwhile, TAP was spatulated into a creamy consistency by mixing 50 mg each of MET, CIP, and MINO with 1 ml sterile DI water, loaded into a plastic syringe and applied into the root canal space. To maintain a humid environment and prevent dehydration of the medications (tubular 3D constructs and TAP), a damp cotton ball saturated with 50 μl of DI water was placed on top of each dentin slice.[29] The medications were allowed to act for 1 week in an incubator at 37°C.

Assessment of antimicrobial efficacy via CLSM and SEM.

To assess the antimicrobial efficacy, two well-established quantitative and qualitative methods were used: confocal laser scanning microscopy (CLSM) and SEM, respectively. For CLSM analysis, 4 dentin slices from each group were stained using fluorescent LIVE/DEAD BacLight Bacterial viability Kit L-7012 (Molecular Probes, Eugene, OR, USA) composed of SYTO 9 and propidium iodide (PI) dyes. Two random areas in each dentin slice were analyzed using a mosaic technique with 3D reconstruction, wherein 9 subareas (300 × 300 μm) were merged, totaling 18 areas per sample (Fig. 2B). The areas were selected starting from the root canal space toward the cementum side for imaging on CLSM using a 40 × lens (Leica SP2 CL5Mt, Leica Microsystems Inc., Heidelberg, Germany). The sequence of segments through the depth of tissue (Z-stacks) was collected by using optimal step size settings (0.35 μm); the images were composed of 512 × 512 pixels and were evaluated and quantified using a dedicated software (Imaris 7.2 software, Bitplane Inc., St. Paul, MN, USA). The excitation emission maxima for the dyes were approximately 480/500 nm for SYTO 9 and 490/635 nm for PI, respectively. The percentages of live/dead bacteria were compared to establish statistical significance in differences of dead bacterial cells between treatment groups using a mixed-model ANOVA, with a fixed effect for group and a random effect for sample, to account for measurements at multiple areas on each specimen.[31] All tests were performed with an alpha level of 5%.

For SEM analysis, the dentin slices were carefully removed from the wells of 24-well culture plates using sterile forceps and gently washed with PBS to remove non-adherent bacteria. Next, they were fixed in 2.5% glutaraldehyde for 24 h and dehydrated in increasing concentrations of alcohol solutions. To visualize bacterial presence/absence, the dentin slices were split in the middle and mounted face-up on Al stubs, sputter coated with Au-Pd prior to imaging.[31,32]

Periapical lesion induction, disinfection and evoked bleeding.

The antimicrobial efficacy of the tubular triple antibiotic-eluting 3D construct (TA-3D$_C$) and regenerative capacity when combined with the evoked bleeding method (i.e., periapical tissue laceration) was investigated *in vivo* using a canine model of periapical disease (Fig. 3).

All animal procedures followed the ARRIVE guidelines for reporting animal research and were in accordance to the procedures of local Institutional Animal Care and Use Committee (IACUC, Indiana University Purdue University at Indianapolis). Ten immature permanent double-rooted upper and lower premolars from one male purpose-bred (Marshall Farms BioResources, North Rose, NY, USA) beagle dog aged ~ 4 months were selected for this IACUC approved study (#DS0000972R). The dog was housed with regulated light and temperature, and fed chow (3×/day) and water ad libitum. Radiographs were taken to confirm incomplete root development (Fig. 3A), that is open apices and teeth were randomly assigned into the following groups: TA-3D$_C$ (n=4), TAP formulated (GreenLeaf Apothecary, Fishers, IN, USA) based on equal parts of MET, CIP, and MINO at 1g/ml (n=4), positive control (infected—restored no further treatment, n=1) and negative control (untouched—normal healthy pulp, n=1) for comparison purposes of development. Briefly, three interventions, under general anesthesia, were conducted sequentially, i.e., periapical lesion induction, disinfection, and EB.

Induction of periapical disease.

Prior to establishing periapical lesions, an injection of acepromazine/butorphanol was given intravenously (2–8 mg/kg) preceding general anesthesia induction with propofol. The animal was intubated and maintained in isoflurane (Abbot Laboratories, Libertyville, IL, USA). The pulp tissues of all experimental premolar teeth were exposed with a #2 round carbide dental bur (DENTSPLY International, York, PA, USA) under irrigation and local anesthesia (bupivacaine plain 0.5%; Abbott Laboratories). A sterile #40 stainless steel endodontic hand file (Dentsply Maillefer, Johnson City, TN) was used to disrupt but not remove the pulp tissue (Fig. 3B). Then, sterile sponges were soaked in 0.9% NaCl (Baxter Healthcare Corp., Deerfield, IL, USA) mixed with supragingival plaque scaled from the dogs' teeth (Fig. 3C) prior to placement into the pulp chamber.[34,35] Teeth were left open (non-restored) to the oral cavity. Post-operation, the animal was given analgesics (Torbugesic 0.2 mg/kg, Butorphanol Tartrate; Fort Dodge Animal Health, Fort Dodge, IA, USA) and monitored by the Animal Care Facility staff and a veterinary professional at Indiana University.

Disinfection strategy.

Upon radiographical confirmation of periapical lesion (4 weeks after induction), under the anesthesia/analgesia protocol described above, the teeth were re-entered under aseptic conditions of rubber dam isolation in addition to surface disinfection with Peridex™ (chlorhexidine gluconate 0.12%, 3M ESPE Dental Products, St. Paul, MN, USA) and 2% iodine tincture (Humco, Texarcana, TX, USA). Following sponge removal, the canals of all treated infected teeth were flushed with 10 ml of 1.5% of NaOCl using the EndoVac™ (Kerr Co., Orange, CA, USA) negative pressure apical irrigation system and dried with sterile paper points (Dentsply Maillefer) (Fig. 3D). Mechanical instrumentation was not performed

in the canals prior to placement of the tubular TA-3D$_C$ (~ 2.5 mg of the three antibiotics per construct) or the triple antibiotic paste. A mixture (1 g/ml) containing equal parts of MET, CIP, and MINO pre-mixed with sterile saline (TAP) and loaded into a plastic syringe was injected into the canals (Fig. 3E). Meanwhile, previously sterilized TA-3D$_C$ (Fig. 3F) were sized to the desired length and press-fitted in the canal spaces using sterile forceps (Fig. 3G). Care was taken to select constructs that made intimate contact with the root canal walls upon forceps insertion. All treated teeth were sealed with a sterile sponge and temporarily restored with a zinc oxide/calcium sulfate-based material (Cavit, 3M ESPE).

Evoked bleeding.

After 4 weeks, under general anesthesia and similar conditions of asepsis and local nerve blocking, the restorative material and sponges were removed under rubber dam isolation from all experimental teeth (TA-3D$_C$ and TAP). The antibiotic mixture was gently irrigated from the canals with 20 ml of 1.5% NaOCl using EndoVac™ to minimize the chance of extrusion of irrigants into the periapical space. Next, the canals were flushed with 20 ml of sterile saline, followed by 20 ml of 17% EDTA irrigation and dried with sterile paper points. To evoke bleeding, a sterile #30 stainless steel pre-curved K-file (Dentsply Maillefer) was introduced 2 mm past the apical foramen to allow blood invasion to the level of the CEJ. A resorbable collagen-based matrix (Collagen Tape, Zimmer Dental, Carlsbad, CA, USA) was placed over the blood clot. These teeth were finally closed with a double coronal seal of white MTA (Dentsply, Tulsa, OK, USA) and light-cured resin composite (A3 Filtek Z250, 3M ESPE) as per the manufacturers' instructions.

Tissue harvest and assessment.

After 3 months of the EB procedure the animal was sacrificed under general anesthesia with intravenous injection of 30 mg/kg pentobarbital (Butler Company, Columbus, OH) and tissues were harvested for histology. The jaw blocks with the involved teeth were dissected and fixed in formaldehyde (Fisher Scientific). After removal of all soft tissue and excess hard tissue from the jaw blocks, the specimens were decalcified with Immunocal (Decal Chemical Corporation, Tallman, NY) for 2 months, with 4 changes of the solution during that time period. The specimens were then washed with distilled water, immersed in 70% ethyl alcohol, dehydrated through ascending gradations of ethanol, embedded in paraffin, and sectioned (5 μm) longitudinally through the apical foramen of the roots on a Leica Jung RM2045 (Leica Microsystems, Wetzlar, Germany) microtome followed by hematoxylin-eosin (H&E) staining. Light microscopy was performed at different magnifications to identify the presence/absence of vital tissues and the overall regenerative capacity of the combined disinfection strategy and EB method.

RESULTS AND DISCUSSION

Characterization of tubular 3D triple antibiotic-eluting constructs.

In the present work, we synthesized a clinically practical biodegradable tubular 3D triple antibiotic-eluting construct and assessed its disinfection potential both *in vitro* and *in vivo*. Regardless of the presence of the antibiotics, the fibrous mats exhibited open porosity and interconnected structures formed by randomly oriented non-woven fibers (Fig. 4A). FTIR

chemical analysis revealed incorporation of the three antibiotics into the electrospun fibers, since their related peaks were observed in the spectra (Fig. 4B). A submicron fiber diameter was observed for both antibiotic-free [1026.1 (320.6 – 2295.2 nm)] and triple antibiotic-eluting fibers [898.5 (625.7 – 1799 nm)] although a more homogeneous fiber distribution was noticed in the latter (Fig. 4C). It is likely that the triple antibiotic-containing polymer (PDS) solution was more hydrophilic than the antibiotic-free counterpart, thereby making the PDS less viscous. This may have contributed to the narrower pore sizes of the less viscous triple antibiotic-containing PDS solution during electrospinning.[36]

Mechanical performance of antibiotic-free fibers and triple antibiotic-eluting fibers, under dry and wet conditions showed that antibiotic-free nanofiber is stronger and has moderate flexibility regardless of the condition tested (Fig. 4D). However, the incorporation of antibiotics at the concentration used here (35 wt.% of antibiotics relative to the total polymer weight) seemed to negatively affect the mechanical properties of the fibers, particularly stretchability (elongation at break). We hypothesize that while antibiotic incorporation may have increased fibers' hydrophilicity, it may also have inadvertently rendered the fibers more easily degradable by enhanced hygroscopic and hydrolytic parameters, which may explain the significant strength reduction.[37] It should be noted that under dry condition, Young's modulus of the triple antibiotic-eluting fibers was as high as the antibiotic-free counterpart (Fig. 4D), suggesting that the antibiotics did not compromise rigidity characteristics of the fibers. Indeed, polar groups found within the molecules of the antibiotics could contribute to hydrogen bonding with the polymer system, thus increasing the modulus. Conversely, the modulus was reduced nearly 10-fold after hydration reduction when compared to the dry samples, indicating that hydrolysis was more intense within the triple antibiotic-eluting fibers even after minimal (24 h) hydration. Although this finding may be viewed as a negative outcome, the fabricated tubular TA-3D$_C$ possesses a biodegradable feature that allows the fibers to progressively degrade in order to ensure their antimicrobial effect. Moreover, since it is desirable for the antibiotics to be released into the root canal, it is reasonable to assume that by degrading the fibers, the antibiotics would be successively released to the medium, thereby ensuring proper root canal disinfection. Consistent with these results, our previous work demonstrated an initial burst release within the first 24 h followed by a sustained maintenance of the antimicrobial effects over 2 weeks.[24,25,31] Taken together, the lower mechanical performance of the triple antibiotic-eluting fibers, when compared to the antibiotic-free counterpart, cannot be considered a clinical limitation, since complete construct degradation is desired for the disinfection strategy proposed here.

Antimicrobial properties against *A. naeslundii* biofilm formed inside dentinal tubules.

Over the past several years, our group has demonstrated unequivocally the antimicrobial efficacy of antibiotic-eluting electrospun polymer nanofibers against endodontic-related biofilms formed on human dentin involving mono-(*E. faecalis, A. naeslundii*, or *P. gingivalis*) and dual-bacterial species (*E. faecalis* and *A. naeslundii*).[27,31,32,38] Although data from these studies showed significant bacterial elimination by the triple antibiotic-eluting nanofibers, the infected-dentin models and the application methods used (antibiotic-eluting nanofibers over infected dentin) did not mimic the clinical scenario or the root canal anatomy. Moreover, considering that long-term intracanal infection generally involves

bacterial penetration deep inside the dentinal tubules, our group adapted a previously established method[33] of centrifuging root canal segments to induce *A. naeslundii* biofilm formation inside dentinal tubules. Another major novelty is the proposed patient-specific (constructs sizeable both in length and diameter) drug delivery system, which involved the prototyping of tubular TA-3D$_C$ that fit smoothly into the root canal space upholding a close contact to the dentin walls and consequently the biofilm and ensuring maximum antimicrobial activity, even at great depths into the dentinal tubules. The method for biofilm formation used in this study successfully allowed the ingrowth of *A. naeslundii* into the dentinal tubules. Table I summarizes the results of the bacterial viability for all groups. Figure 5 shows the CLSM scans and 3D reconstructions of the obtained images, as well as the percentage (%) values for dead and live bacteria. The control group (untreated 7-day biofilm) showed a dense penetration of *A. naeslundii* deep in the dentinal tubules with a dominant green color indicating the robust presence of viable *A. naeslundii*. Bacterial viability for this group was between 99.88 and 99.99%. The antibiotic-free tubular 3D constructs (AF-3D$_C$) also showed a high percentage of bacterial viability (98.01 % — 99.34 %). The proportion of dead bacterial cells for slices treated with the novel triple antibiotic-eluting constructs (TA-3D$_C$) ranged from 99.1 % to 99.94 %, which was significantly different compared to the AF-3D$_C$ ($p < 0.05$). The group treated with TAP showed a 100 % reduction in bacterial viability (Fig. 5). However, there was no statistically significant difference between the data from the TAP and the TA-3D$_C$ groups. Consistent with the CLSM results, SEM imaging also demonstrated the penetration of *A. naeslundii* into the dentinal tubules from the root canal side after centrifugation and incubation of these specimens. SEM images (Fig. 6) showed bacterial presence inside the dentinal tubules in the day 7 biofilm control (Fig. 6B) and the AF-3D$_C$ (Fig. 6C). Both the TAP (Fig. 6D) and the tubular TA-3D$_C$ (Fig. 6E) treated groups showed mostly bacterial-free dentinal tubules. Taken together, these supporting evidence led our team to test the tubular TA-3D$_C$ *in vivo* using a dog model of periapical disease.

Disinfection and regenerative potential — *In vivo* study.

Complete apical closure of the root could be clearly observed in the negative control, i.e., the group in which perapical disease was not instated (Fig. 7A). This outcome is indeed expected, since in the absence of infection, the root of immature teeth may develop continuously until proper thickening of the canal walls, with subsequent apical closure. As shown in Fig. 7B, the pulp tissue within the root canal of the non-infected (negative control) tooth was comprised of a healthy loose connective tissue and erythrocyte-filled blood vessels filled with red blood cells; odontoblasts were also observed at the pre-dentin layer. According to several studies, the maturation of permanent teeth is a physiological process that depends on the survival of Hertwig's epithelial root sheath (HERS) and the apical papilla.[15]

We successfully developed periapical inflammatory disease, as evidenced by the ovoid-shaped lesion around the open root apex (Fig. 7C). Histopathologic examination revelared the presence of a dense inflammatory infiltrate around the apical area (Fig. 7D), which probably destroyed HERS and the apical papilla.[34,39] Consequently, periapical healing and complete root maturation were hindered. A collection of disorganized pulp tissue remained

in the root canal, suggesting necrosis of that tissue due to bacterial infection. Odontoblasts and blood vessels could not be observed at that stage, thus indicating an unlike scenario for dentin formation and pulp survival.

It is well established that the presence of bacteria plays a negative role in regenerative endodontic procedures, preventing dentin formation and periapical healing.[40] To properly ablate infection, TAP has been effectively used as an intracanal medication prior to the EB clinical procedure. As evident in Fig. 8A (TAP-treated group), the root apex of the tooth was almost completely closed, indicating the formation of new tissues and root maturation. This finding corroborates other studies.[13,15,41] However, it is possible to note some differences between the healing process obtained by the regenerative endodontic procedure using TAP and the physiological process of root maturation seen in the non-infected group (negative control). First, it seems that the former allows apex closure by forming an osteodentin-like tissue, compared to the dentin tissue seen in the non-infected group (negative control). Indeed, a hollow hard tissue is clearly observed at the apical area of the root apex, suggesting that cells other than odontoblasts, participated in the healing process and apical closure. Irrigation solutions (NaOCl) and intracanal medication (calcium hydroxide and antibiotics) used in endodontics may both destroy part of the residual vital apical pulp tissue due to cytotoxic effects[19], such that odontoblasts would have been severely compromised. On the other hand, the apical papilla usually survives the toxic action of those solutions/medicaments, thus becoming the most viable source for cell proliferation and differentiation under regenerative endodontic circumstances.[14,41] Studies have already reported that stem cells from the apical papilla have more potential to differentiate into odontoblast-like cells when compared to stem cells from the dental pulp, but only upon specific signaling induction.[42,43] Thus, it may be assumed that stem cells from the apical papilla may have differentiated into osteoblast- and odontoblast-like cells in our study, allowing apex closure, but through the formation of a hollow hard tissue/osteodentin (Fig. 8A). It is also worth noting that despite the absence of any periapical lesion around the root apex, a concise and well-localized inflammatory infiltrate could be observed at the periapical area of the TAP-treated tooth (Fig. 8B), suggesting that residual live bacteria remained external to the root apex, or that some residual antibiotic components from TAP were provoking tissue inflammation, as complete TAP removal from the root canal has shown to be a difficult task.[20]

Alternative strategies to TAP have been recently proposed, including the use of electrospun fibers containing 500-fold lower concentrations of the three antibiotics found in TAP (1 g/ml). One of the main advantages of using fibers as a drug delivery system relies on the minimal cytotoxic effect combined with the antimicrobial effect similar to that of TAP. In this study, one should appreciate that the proposed tubular 3D triple antibiotic-eluting construct (TA-$3D_C$) greatly reduced bacterial infection, thereby allowing tissue formation and complete apical root closure (Fig. 8C). Nevertheless, and similarly to the TAP-treated tooth, the new tissue formed during root maturation was more consistent with an osteodentin-like tissue. Once again, this may have occurred due to the differentiation of stem cells from the apical papilla into osteoblast- and odontoblast-like cells.[14] Interestingly, a chronic inflammatory process could be seen at the periapical area of the root apex (Fig. 8D), although without the presence of an organized biofilm structure. It can be assumed that even

with reduced antibiotic concentration, the TA-3D$_C$ may provoke an inflammatory reaction, although less intense than that seen in the TAP-treated teeth.

Here, we demonstrated *in vivo* the feasibility and overall role of a patient-specific tubular 3D triple antibiotic-eluting construct as an intracanal drug delivery system in a dog model of periapical disease. Noteworthy, although one hesitates to state categorically that the 3D construct is completely bonded to the tooth at the apical area, as our group continues working on this development, we plan to investigate the potential of adding cytocompatible and radiopaque nanoparticles as a contrast agent for X-ray imaging. Overall, the histological data showed that the association of a biocompatible disinfection strategy with periapical tissue laceration to evoke bleeding in a bacteria-free niche led to an appropriate environment that displayed apical root closure and the ingrowth of a thin layer of osteodentin-like tissue into the root canal. Collectively, although the establishment of an apical hard tissue barrier by itself may not be the ideal outcome, this method allows further studies by combining the proposed disinfection strategy with injectable biomaterial scaffolds loaded or not with stem cells and/or growth factors aiming to amplify the likelihood of achieving predictable regeneration of the pulp-dentin complex.

CONCLUSION

Electrospinning was used to fabricate tubular 3D drug delivery constructs comprising polydioxanone and three antibiotics (metronidazole, ciprofloxacin, and minocycline) at a much lower concentration than in the triple antibiotic paste (TAP) used clinically during the disinfection step of the evoked bleeding method. The 3D construct was designed to smoothly fit within the individual anatomy of immature teeth, i.e., a parallel and tubular thin root dentin wall. Biofilm was also successfully introduced into dentinal tubules, mimicking the clinical condition of an infected tooth. The tubular 3D triple antibiotic-eluting drug delivery constructs were effective in ablating intracanal biofilm in a similar fashion to the well-established TAP.

ACKNOWLEDGEMENTS

The authors deny any conflicts of interest related to this study. We thank James Steven Driver (Indiana University School of Dentistry, Endodontics Department) and Carol L. Bain (Indiana University School of Medicine, Indianapolis, IN, USA) for their invaluable assistance during dog surgery and histology processing, respectively. M.C.B. acknowledges the National Institutes of Health (NIH)/National Institute of Dental and Craniofacial Research (NIDCR) (Grants K08DE023552 and R01DE026578). The content is solely the responsibility of the authors and does not necessarily represent the official views of the National Institutes of Health.

REFERENCES

1. Kim SG, Zheng Y, Zhou J, Chen M, Embree MC, Song K, et al. Dentin and dental pulp regeneration by the patient's endogenous cells. Endod Topics 2013;28:106–117. [PubMed: 24976816]
2. Nakashima M, Akamine A. The application of tissue engineering to regeneration of pulp and dentin in endodontics. J Endod 2005;31:711–8. [PubMed: 16186748]
3. Diogenes A, Ruparel NB. Regenerative endodontic procedures: clinical outcomes. Dent Clin North Am 2017;61:111–125. [PubMed: 27912813]
4. Dye BA, Thornton-Evans G, Li X, Iafolla T. Dental caries and tooth loss in adults in the United States, 2011–2012. NCHS Data Brief 2015;197. [PubMed: 25973996]

5. Lee JY, Vann WF Jr, Sigurdsson A. Management of avulsed permanent incisors: a decision analysis based on changing concepts. Pediatr Dent 2001;23:357–60. [PubMed: 11572500]
6. Conde MCM, Chisini LA, Sarkis-Onofre R, Schuch HS, Nör JE, Demarco FF. A scoping review of root canal revascularization: relevant aspects for clinical success and tissue formation. Int Endod J 2017;50:860–874. [PubMed: 27770435]
7. Banchs F, Trope M. Revascularization of immature permanent teeth with apical periodontitis: new treatment protocol? J Endod 2004;30:196–200. [PubMed: 15085044]
8. Cvek M Prognosis of luxated non-vital maxillary incisors treated with calcium hydroxide and filled with gutta-percha. A retrospective clinical study. Endod Dent Traumatol 1992;8:45–55. [PubMed: 1521505]
9. Damle SG, Bhattal H, Loomba A. Apexification of anterior teeth: a comparative evaluation of mineral trioxide aggregate and calcium hydroxide paste. J Clin Pediatr Dent 2012;36:263–8. [PubMed: 22838228]
10. Ostby BN. The role of the blood clot in endodontic therapy. An experimental histologic study. Acta Odontol Scand 1961;19:324–353. [PubMed: 14482575]
11. Iwaya SI, Ikawa M, Kubota M. Revascularization of an immature permanent tooth with apical periodontitis and sinus tract. Dent Traumatol 2001;17:185–187. [PubMed: 11585146]
12. Lovelace TW, Henry MA, Hargreaves KM, Diogenes A. Evaluation of the delivery of mesenchymal stem cells into the root canal space of necrotic immature teeth after clinical regenerative endodontic procedure. J Endod 2011;37:133–138. [PubMed: 21238791]
13. Nagy MM, Tawfik HE, Hashem AA, Abu-Seida AM. Regenerative potential of immature permanent teeth with necrotic pulps after different regenerative protocols. J Endod 2014;40:192–198. [PubMed: 24461403]
14. Shimizu E, Jong G, Partridge N, Rosenberg PA, Lin LM. Histologic observation of a human immature permanent tooth with irreversible pulpitis after revascularization/regeneration procedure. J Endod 2012;38:1293–1297. [PubMed: 22892754]
15. Peng C, Zhao Y, Wang W, Yang Y, Qin M, Ge L. Histologic findings of a human immature revascularized/regenerated tooth with symptomatic irreversible pulpitis. J Endod 2017;43:905–909. [PubMed: 28416306]
16. Rosa V, Zhang Z, Grande RH, Nör JE. Dental pulp tissue engineering in full-length human root canals. J Dent Res 2013;92:970–975. [PubMed: 24056227]
17. Zhang Z, Nör F, Oh M, Cucco C, Shi S, Nör JE. Wnt/β-catenin signaling determines the vasculogenic fate of postnatal mesenchymal stem cells. Stem Cells 2016;34:1576–87. [PubMed: 26866635]
18. Nakashima M, Iohara K, Murakami M, Nakamura H, Sato Y, Ariji Y, Matsushita K. Pulp regeneration by transplantation of dental pulp stem cells in pulpitis: a pilot clinica study. Stem Cell Res Ther 2017;8:(1), 61. doi: 10.1186/s13287-017-0506-5. [PubMed: 28279187]
19. Ruparel NB, Teixeira FB, Ferraz CC, Diogenes A. Direct effect of intracanal medicaments on survival of stem cells of the apical papilla. J Endod 2012;38:1372–1375. [PubMed: 22980180]
20. Berkhoff JA, Chen PB, Teixeira FB, Diogenes A. Evaluation of triple antibiotic paste removal by different irrigation procedures. J Endod 2014;40:1172–1177. [PubMed: 25069927]
21. Galler KM, Buchalla W, Hiller KA, Federlin M, Eidt A, Schiefersteiner M, et al. Influence of root canal disinfectants on growth factor release from dentin. J Endod 2015;41:363–368. [PubMed: 25595468]
22. Albuquerque MT, Valera MC, Nakashima M, Nör JE, Bottino, MC. Tissue-engineering-based strategies for regenerative endodontics. J Dent Res 2014;93:1222–31. [PubMed: 25201917]
23. Albuquerque MT, Nagata JY, Diogenes AR, Azabi AA, Gregory RL, Bottino MC. Clinical perspective of electrospun nanofibers as a drug delivery strategy for regenerative endodontics. Curr Oral Health Rep 2016;3:209–220.
24. Bottino MC, Kamocki K, Yassen GH, Platt JA, Vail MM, Ehrlich Y, et al. Bioactive nanofibrous scaffolds for regenerative endodontics. J Dent Res 2013;92:963–969. [PubMed: 24056225]
25. Palasuk J, Kamocki K, Hippenmeyer L, Platt JA, Spolnik KJ, Gregory RL, et al. Bimix antimicrobial scaffolds for regenerative endodontics. J Endod 2014;40:1879–84. [PubMed: 25201643]

26. Kamocki K, Nör JE, Bottino MC. Dental pulp stem cell responses to novel antibiotic-containing scaffolds for regenerative endodontics. Int Endod J 2015;48:1147–1156. [PubMed: 25425048]
27. Pankajakshan D, Albuquerque MT, Evans JD, Kamocka MM, Gregory RL, Bottino MC. Triple antibiotic polymer nanofibers for intracanal drug delivery: effects on dual species biofilm and cell function. J Endod 2016;42:1490–1495. [PubMed: 27663615]
28. Bottino MC, Yassen GH, Platt JA, Labban N, Windsor LJ, Spolnik KJ, et al. A novel three-dimensional scaffold for regenerative endodontics: materials and biological characterizations. J Tissue Eng Regen Med 2015;9(11):E116–123. [PubMed: 23475586]
29. Porter ML, Münchow EA, Albuquerque MT, Spolnik KJ, Hara AT, Bottino MC. Effects of novel 3-dimensional antibiotic-containing electrospun scaffolds on dentin discoloration. J Endod 2016;42:106–12. [PubMed: 26602451]
30. Münchow EA, Albuquerque MT, Zero B, Kamocki K, Piva E, Gregory RL, et al. Development and characterization of novel ZnO-loaded electrospun membranes for periodontal regeneration. Dent Mater 2015;31:1038–1051. [PubMed: 26116414]
31. Albuquerque MT, Ryan SJ, Münchow EA, Kamocka MM, Gregory RL, Valera MC, et al. Antimicrobial effects of novel triple antibiotic paste-mimic scaffolds on Actinomyces naeslundii biofilm. J Endod 2015;41:1337–1343. [PubMed: 25917945]
32. Albuquerque MT, Valera MC, Moreira CS, Bresciani E, de Melo RM, Bottino MC. Effects of ciprofloxacin-containing scaffolds on Enterococcus faecalis biofilms. J Endod 2015; 41:710–714. [PubMed: 25698261]
33. Ma J, Wang Z, Shen Y, Haapasalo M. A new noninvasive model to study the effectiveness of dentin disinfection by using confocal laser scanning microscopy. J Endod 2011:37:1380–1385. [PubMed: 21924186]
34. Wang X, Thibodeau B, Trope M, Lin LM, Huang GT. Histologic characterization of regenerated tissues in canal space after the revitalization/revascularization procedure of immature dog teeth with apical periodontitis. J Endod 2010;36:56–63. [PubMed: 20003936]
35. Yamauchi N, Yamauchi S, Nagaoka H, Duggan D, Zhong S, Lee SM, et al. Tissue engineering strategies for immature teeth with apical periodontitis. J Endod 2011;37:390–397. [PubMed: 21329828]
36. Dargaville BL, Vaquette C, Rasoul F, Cooper-White JJ, Campbell JH, Whittaker AK. Electrospinning and crosslinking of low-molecular-weight poly(trimethylene carbonate-co-(L)-lactide) as an elastomeric scaffold for vascular engineering. Acta Biomater 2013;9:6885–6897. [PubMed: 23416575]
37. Ferracane JL. Hygroscopic and hydrolytic effects in dental polymer networks. Dent Mater 2006;22:211–222. [PubMed: 16087225]
38. Albuquerque MT, Evans JD, Gregory RL, Valera MC, Bottino MC. Antibacterial TAP-mimic electrospun polymer scaffold: effects on P. gingivalis-infected dentin biofilm. Clin Oral Investig 2016;20:387–393.
39. da Silva LA, Nelson-Filho P, da Silva RA, Flores DS, Heilborn C, Johnson JD, et al. Revascularization and periapical repair after endodontic treatment using apical negative pressure irrigation versus conventional irrigation plus triantibiotic intracanal dressing in dogs' teeth with apical periodontitis. Oral Surg Oral Med Oral Pathol Oral Radiol Endod 2010;109:779–87. [PubMed: 20416538]
40. Verma P, Nosrat A, Kim JR, Price JB, Wang P, Bair E, et al. Effect of residual bacteria on the outcome of pulp regeneration in vivo. J Dent Res 2017;96:100–106. [PubMed: 27694153]
41. Palma PJ, Ramos JC, Martins JB, Diogenes A, Figueiredo MH, Ferreira P, et al. Histologic evaluation of regenerative endodontic procedures with the use of chitosan scaffolds in immature dog teeth with apical periodontitis. J Endod 2017;43:1279–1287. [PubMed: 28577961]
42. Huang GT, Gronthos S, Shi S. Mesenchymal stem cells derived from dental tissues vs. those from other sources: their biology and role in regenerative medicine. J Dent Res 2009;88:792–806. [PubMed: 19767575]
43. Tziafas D, Kodonas K. Differentiation potential of dental papilla, dental pulp, and apical papilla progenitor cells. J Endod 2010;36:781–9. [PubMed: 20416419]

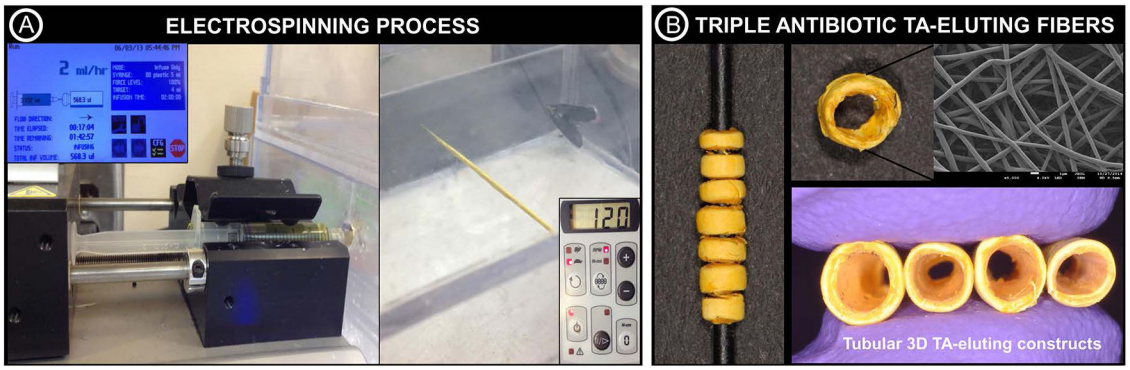

FIGURE 1.

(A) Electrospinning setup used for the fabrication of the tubular 3D triple antibiotic-eluting constructs (TA-$3D_C$), with the following processing parameters: needle-collector distance of 18 cm, flow rate of 2 $mL.h^{-1}$, and voltage of 15–19 kV. (B) TA-$3D_C$ and SEM micrograph (×5000) of the triple antibiotic-eluting nanofibers obtained via electrospinning.

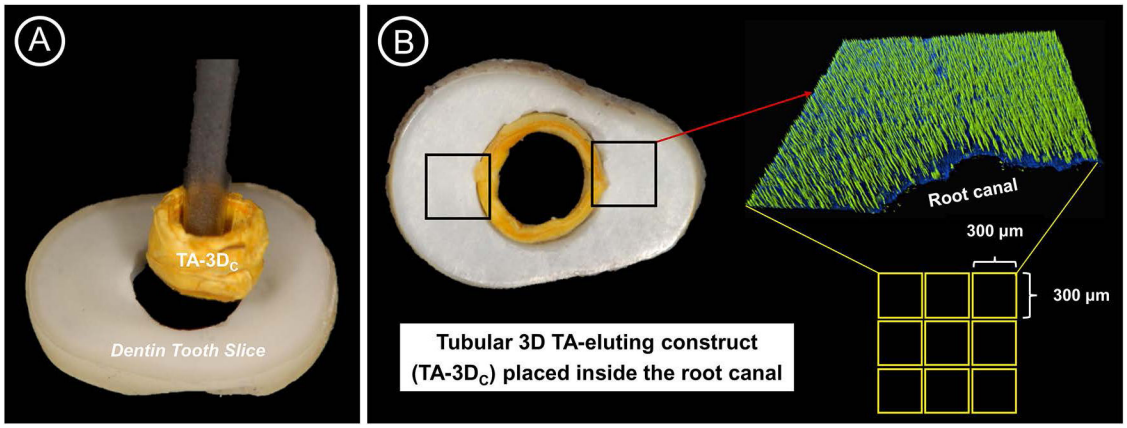

FIGURE 2.

(A) Representative image showing the insertion of the tubular 3D triple antibiotic-eluting construct (TA-3D$_C$) inside the root canal of the dentin tooth slice. (B) Image showing the smooth fitting of the TA-3D$_C$ inside the root canal and the method used (CLSM) to verify its disinfection ability against *A. naeslundii* biofilm.

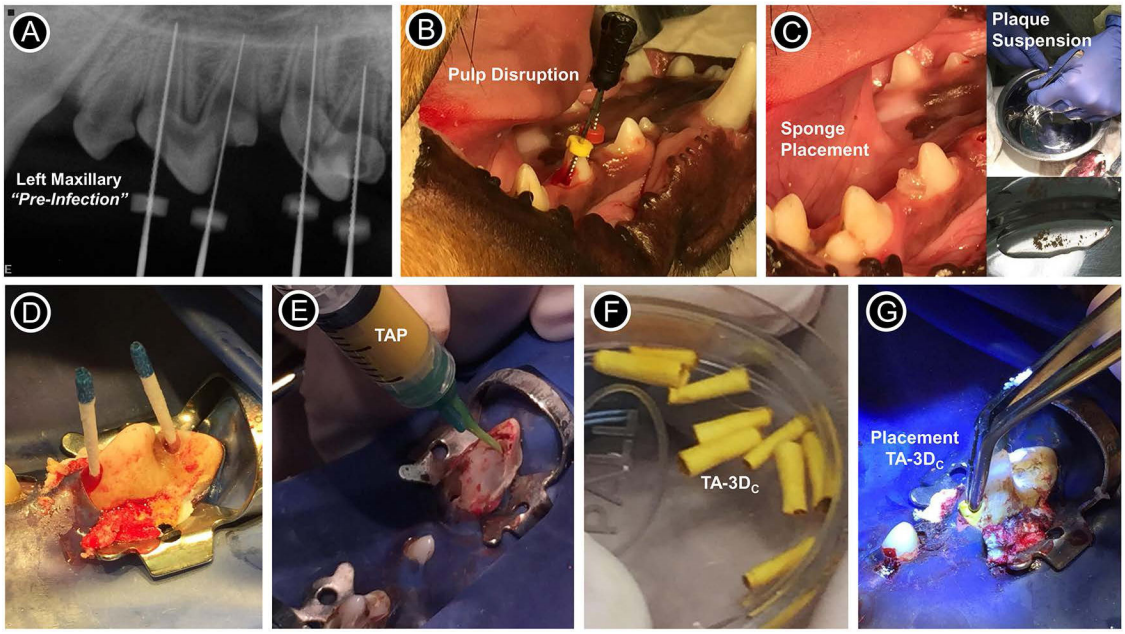

FIGURE 3.

Images showing the periapical lesion induction, disinfection and evoked bleeding procedures performed for the *in vivo* study. (A) Radiograph from the left maxillary of the dog showing the pre-infection scenario of immature permanent teeth with incomplete root development (i.e., open apices). (B) Pulp disruption performed with a sterile #40 stainless steel endodontic hand file. (C) Placement of sterile sponges inside the pulp chamber and inset images showing the plaque suspension (supragingival plaque) that was mixed with the sponges previously soaked in 0.9% NaCl. (D) Following sponge removal, the root canals were flushed with 10 ml of 1.5% of NaOCl and dried with sterile paper points. (E) For TAP group, a mixture (1 g/ml) containing equal parts of metronidazole, ciprofloxacin, and minocycline pre-mixed with sterile saline was loaded into a plastic syringe and injected into the canals; For tubular 3D triple antibiotic-eluting construct (TA-3D$_C$) group, each TA-3D$_C$ was sized to the desired length (F) and press-fitted in the canal spaces using a sterile forceps (G).

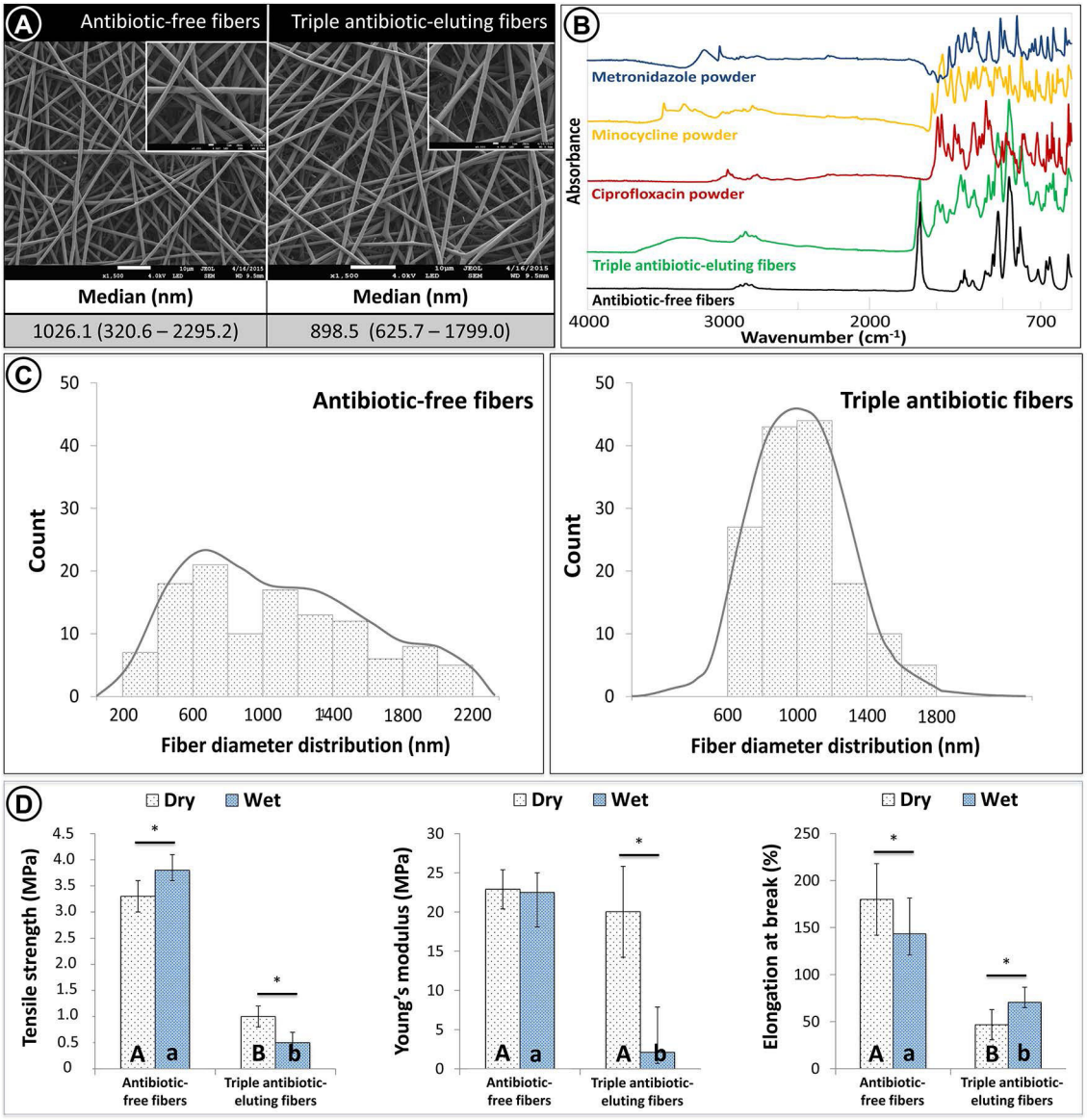

FIGURE 4.

(A) SEM micrographs of antibiotic-free and triple antibiotic TA-eluting fibers, both showing a porous structure and smooth morphology with similar median fiber diameter. (B) FTIR spectra demonstrated antibiotic incorporation into the TA-eluting fibers. (C) Antibiotic-free fibers showed a wider range of diameter distribution (heterogeneous) compared with TA-eluting fibers, which displayed a gaussian distribution (homogeneous). Regarding the mechanical analysis (i.e., tensile strength, Young's modulus, and elongation at break) (D), statistically significant differences between antibiotic-free fibers and TA-eluting fibers were seen (represented by different uppercase [dry condition] and lowercase [wet condition] letters [$P < .05$]). In detail, under dry conditions, the TA-eluting fibers demonstrated lower tensile strength and elongation at break ($P < .05$) when compared with antibiotic-free fibers, although presenting with a similar Young's modulus ($P > .05$). After hydration, lower mechanical properties ($P < .05$) were obtained for the antibiotic-eluting fibers when

compared with the antibiotic-free fibers. Asterisk (*) above bar columns indicates statistically significant difference between dry and wet storage conditions ($P < .05$).

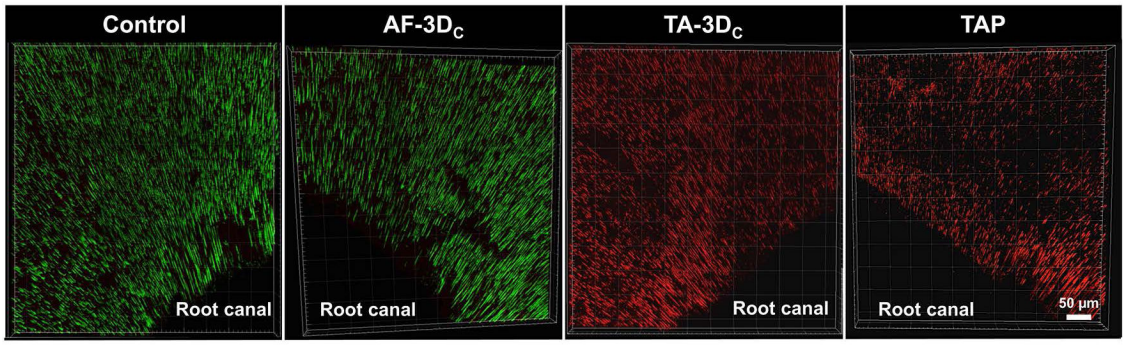

	Groups	N (Areas)	N (Samples)	Min	Max	Median
DEAD	Control	18	4	0.01	0.12	0.03
	AF-3D$_C$	18	4	0.66	1.99	1.2
	TA-3D$_C$	18	4	99.1	99.94	99.8
	TAP	18	4	100	100	100
LIVE	Control	18	4	99.88	99.99	99.97
	AF-3D$_C$	18	4	98.01	99.34	98.77
	TA-3D$_C$	18	4	0.06	0.99	0.21
	TAP	18	4	0	0	0

FIGURE 5.

CLSM macrophotographs of 7-day *A. naeslundii* biofilm growth inside dentinal tubules (control), and infected dentin treated for 7 days with tubular 3D antibiotic-free construct (AF-3D$_C$), tubular 3D triple antibiotic-eluting construct (TA-3D$_C$), or TAP solution. CLSM images were collected from inner root canal walls with a mosaic technique allowing a deeper analysis in sequential illumination mode by using 488-nm and 552-nm laser lines. Fluorescent emission was collected in 2 HyD spectral detectors with filter range set up to 500–550 nm and 590–655 nm for green (SYTO9) and red dye (PI), respectively. Inset Table illustrating median percentage of DEAD and LIVE bacterial cells of each group, demonstrating that TA-3D$_C$ eliminated almost all live cells, not differing from TAP solution.

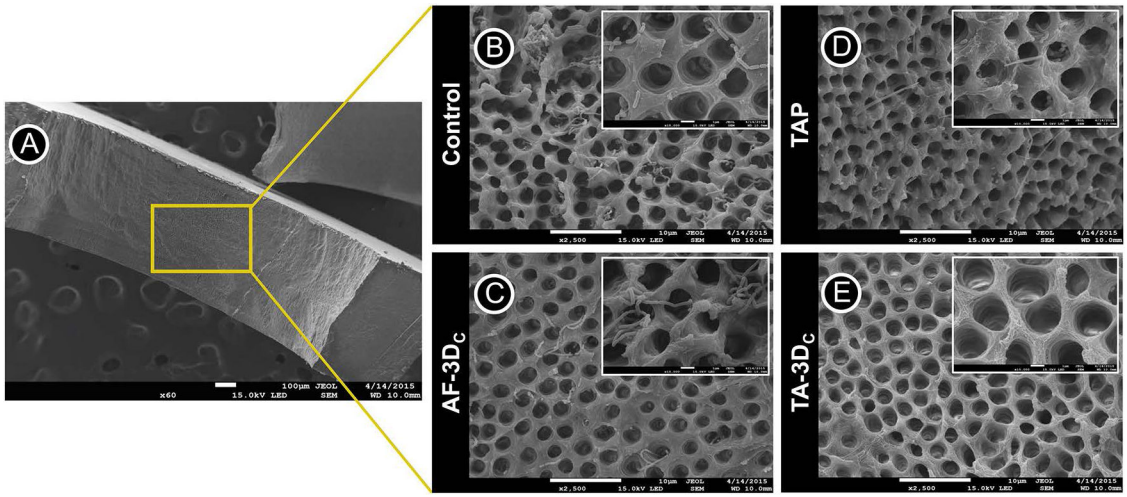

FIGURE 6.

(A) SEM images were obtained from the inner root walls of dentin slices (original magnification ×60). SEM images of *A. naeslundii* biofilm on the dentin surface (control) (B) treated by tubular 3D antibiotic-free construct (AF-3D$_C$) (C), TAP solution (D), and tubular 3D triple antibiotic-eluting construct (TA-3D$_C$) (E) (original magnification ×2500). Control and AF-3D$_C$ group demonstrate viable bacteria on dentin surfaces and inside dentinal tubules. TAP solution and TA-3D$_C$ groups eliminated almost all viable bacteria on dentin surface and inside dentinal tubules.

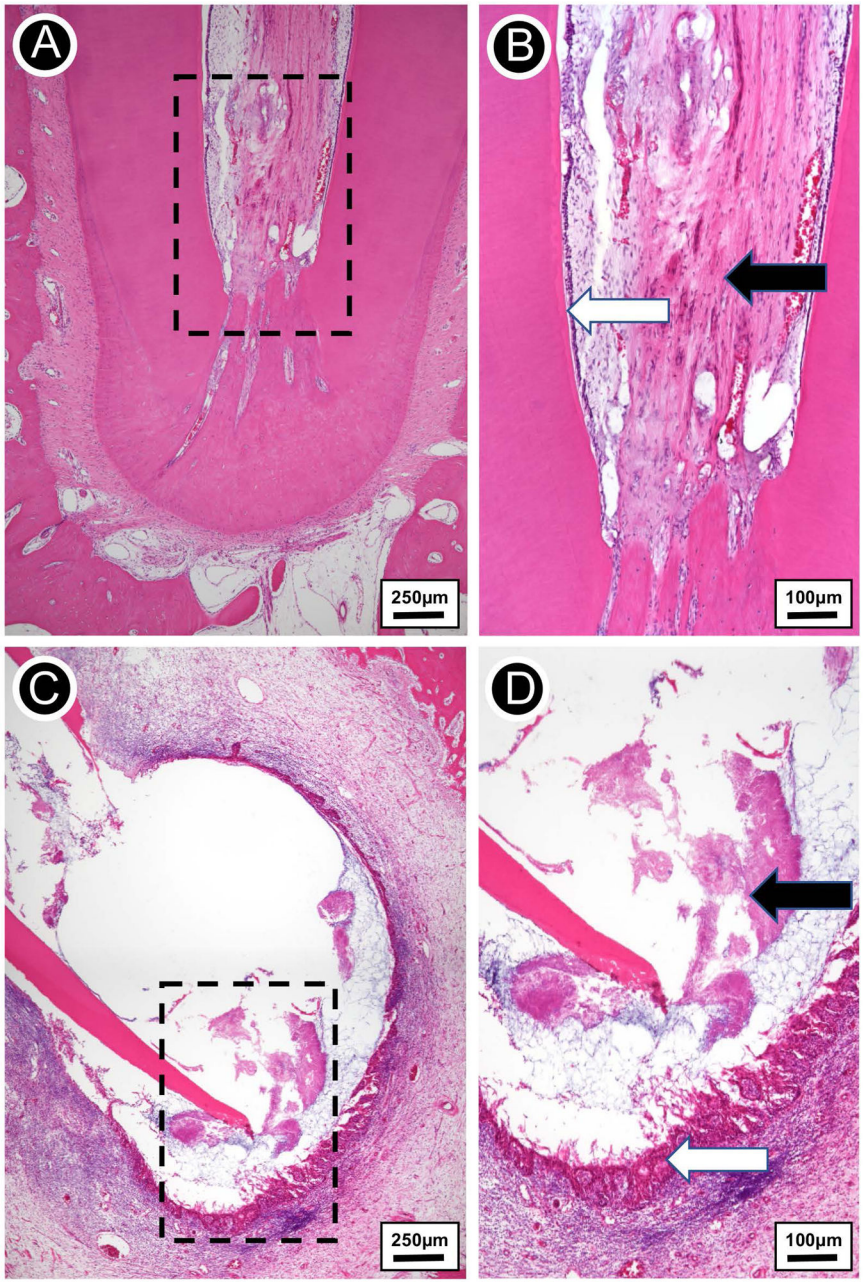

FIGURE 7.

(A) Hematoxylin-eosin stained micrograph of extracted tooth free of infection. (B) Higher magnification view of the rectangular area from *A*. Vital fibrovascular pulp devoid of inflammation (black arrow), with odontoblasts lining the inner dentin (white arrow). (C) Hematoxylin-eosin stained micrograph of extracted infected tooth showing a periapical lesion comprised of lateral and apical root resorption. (D) A detailed view of the rectangular area from *C*. Extensive replacement of alveolar bone by chronically inflamed epithelial-lined granulation tissue (black arrow) and filamentous bacterial colonies (white arrow) at the apical third.

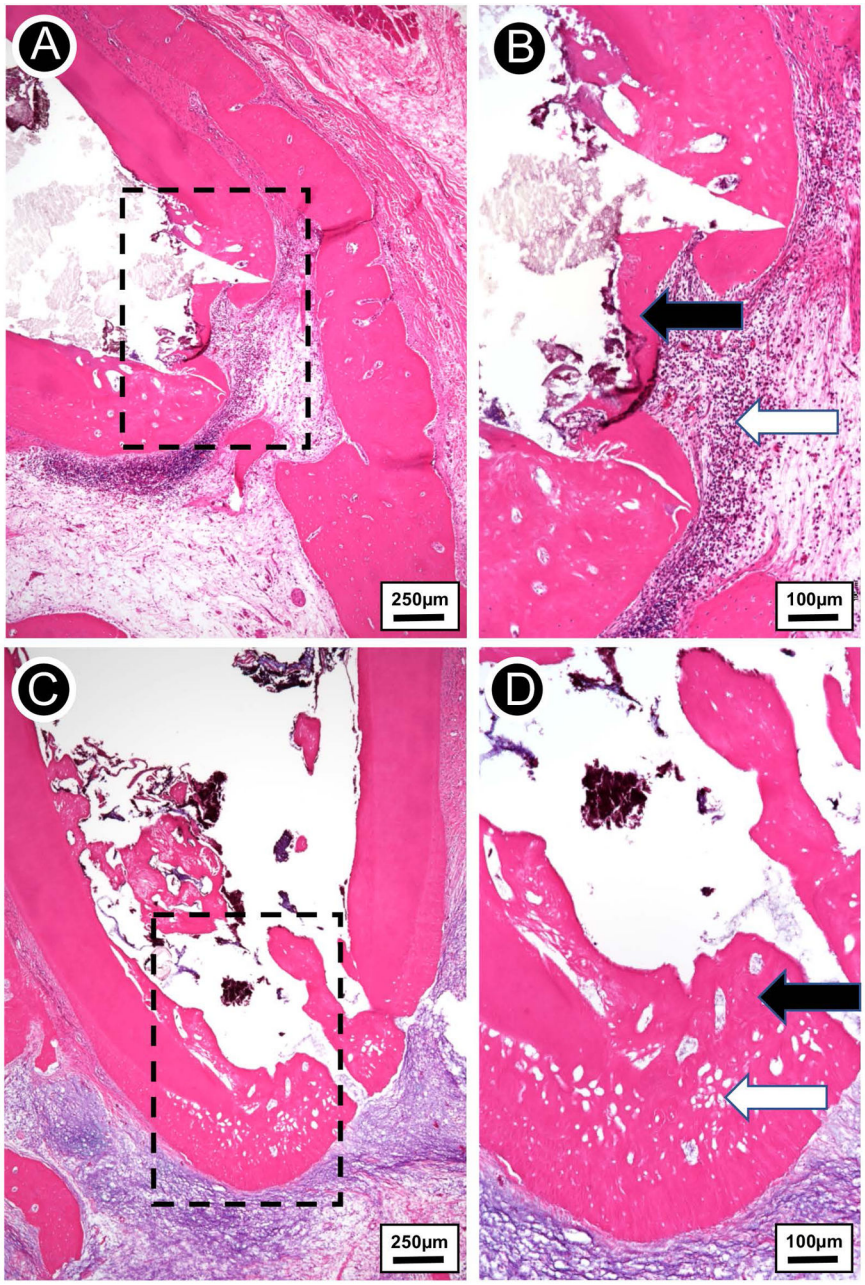

FIGURE 8.

(A) Hematoxylin-eosin stained micrograph of extracted infected tooth treated with TAP solution, showing a thin bridge of apical osteodentin with early periapical bone destruction. (B) Higher magnification view of the rectangular area from *A*. Thin irregular osteodentin bridge at root apex (black arrow) and adjacent chronically inflamed granulation tissue and collections of neutrophils (white arrow). (C) Hematoxylin-eosin stained micrograph of extracted infected tooth treated with the tubular 3D triple antibiotic-eluting construct, showing thick layer of regenerated osteodentin restoring the outline of the root apex. The osteodentin demonstrates cellular inclusions and resembles a combination of bone, osteoid, predentin, and dentin. (D) Higher magnification view of the rectangular area from *C*.

Complete regeneration of apical root structure (thick osteodentin layer; black arrow). The regenerated osteodentin recapitulates the normal root apex outline with well-developed osteodentin containing cellular inclusions (white arrow).